Adhesion of Edible Oils to Food Contact Surfaces

Marie-Caroline Michalski[a], Stéphane Desobry[a,*], Marie-Noëlle Pons[b], and Joël Hardy[a]

[a]Laboratoire de Physico-chimie et Génie Alimentaires, ENSAIA - INPL, 2, 54505 Vandoeuvre-lès-Nancy Cedex, France, and [b]Laboratoire des Sciences du Génie Chimique, 54000 Nancy, France

ABSTRACT: Adhesion of oils and fatty food products to packages is an important storage problem, because it increases product–package interactions that alter quality. Reducing such adhesion would also allow savings in recycling and cleaning processes. The aim of our work was to test if some thermodynamical adhesion models were correlated to edible oils' bulk adhesion as measured experimentally. Food-contact surfaces were low-density polyethylene, polyethylene teraphthalate, stainless steel, and glass. The Young-Dupré equation and five models of adhesion from the literature were used to calculate solids' surface tension and the thermodynamical work of adhesion (Wa). The dispersive, polar, acid-base, and hydrogen surface tension components of oils and solids were calculated. The experimental adhesion, or amount of edible oils remaining on solid surfaces after contact, was found to be correlated to Young-Dupré Wa, involving contact angle measured by specially designed image analysis technique. Two models, involving, respectively, surface tension's hydrogen component and a linear dependence of Wa^p on the liquid polar surface tension component, fitted best with oil bulk adhesion as measured experimentally. Our theoretical approach to fatty food material adhesion seems, so far, consistent to predict global residues of edible oils on solid surfaces.
JAOCS 75, 447–454 (1998).

KEY WORDS: Adhesion models, contact angle, edible oil, food, image analysis, packaging, surface tension.

Adhesion of fatty food materials to surfaces is of high economic importance. Residues remaining on packages increase recycling costs. Food adhesion on equipment and machines also affects industrial cleaning costs, especially for greasy products. Moreover, adhesion to food packaging enhances interactions that may alter the food product and lead to poor product appearance (1).

In general, adhesion is explained by different theories, such as thermodynamics (surface tension, contact angle), mechanics (rugosity, wear), electrostatics, and diffusion, which led to adhesion models. However, most studies concerning food adhesion to surfaces are empirical and related to specific products, such as meat, fish, or dough. Few are concerned with adhesion of fatty food products, as are studies by Checkmareva *et al.* (2). All these studies have not taken into account the existing theoretical adhesion models (3). McGuire and coworkers (4–7) used the thermodynamical adsorption theory of adhesion but for specific food components, such as proteins, rather than for real food products. Concerning food contact surfaces, theoretical adhesion approaches were used by Boulange-Peterman *et al.* (8) for sanitary purposes concerning the adhesion of microorganisms.

The aim of the present study was to show the relationship between the thermodynamic work of adhesion (Wa) and the weight of fatty food remaining on packaging material after drainage flow. This bulk residual weight, which we chose to call experimental adhesion, represents the adhesion plus cohesion amount that is of real industrial concern. Our goal was to see if this global adhesion is also linked to truly interfacial terms, such as the work of adhesion or surface tension parameters.

Wa was calculated from the Young-Dupré equation and five methods from the literature. Oils were chosen for their important cleaning problems because they are particularly difficult to remove from surfaces. Moreover, there may be a model to understand better the behavior of fatty fluid food products. They were also chosen among other fatty foods for their properties such as lack of evaporation and Newtonian rheological behavior. This allowed us to concentrate on thermodynamical parameters.

THERMODYNAMIC ADHESION MODELS

The thermodynamic work of adhesion, Wa, may be defined as the reversible work per unit surface to separate two phases that initially have a common interface. It characterizes the reversible part of the nonequilibrium adhesion work developed in the real process of separation of bodies. Wa is positive for adhesion and may be expressed by a combination of the Young forces equation (9) and the Dupré energy equation (10), leading to:

$$Wa = \gamma_L \cdot (\cos \theta + 1) \qquad [1]$$

where γ_L is the liquid surface tension and θ the contact angle at the solid–liquid interface (Fig. 1). The advantage of this equation is that calculation of Wa is based only on γ_L and θ determination, which is experimentally relatively easy. Wa is

*To whom correspondence should be addressed at Laboratoire de Physico-chimie et Génie Alimentaires, ENSAIA - INPL, 2, avenue de la forêt de Haye, BP 172, 54505 Vandoeuvre-lès-Nancy Cedex, France.
E-mail: desobry@ensaia.u-nancy.fr.

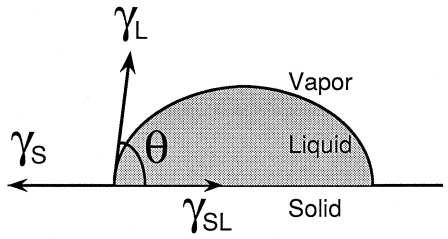

FIG. 1. Definition of contact angle from sessile drop geometry at solid/liquid/vapor triple point. γ_S, γ_L, and γ_{SL} are solid and liquid surface tension and solid-liquid interfacial tension, respectively.

thus calculated with some certainty because this equation is valid for any liquid on any solid surface.

However, some models have been established to express the work of adhesion and understand the role of dispersive, polar, and acid-base forces in the adhesive process. In these models, solid surface tension components, i.e., the additive dispersive, polar, acid-base, or hydrogen contributions to surface tension, must be known. Because currently there is no reliable experimental technique for directly measuring the surface tension of a solid and its components, indirect methods must be used. Particularly, they can be deduced from contact angles of pure standard liquids on the surface of the solid, by using a combination of the Young-Dupré equation and one of the models. Most of these rely on Fowkes' expression of the Wa dispersive part as a geometric mean of the dispersive surface tension's components (11). Five of the most common models were tested in this study.

(i) Owens and Wendt model (12),

$$Wa = 2 \cdot \sqrt{\gamma_S^d \cdot \gamma_L^d} + 2 \cdot \sqrt{\gamma_S^p \cdot \gamma_L^p} \qquad [2]$$

where γ^d and γ^p are surface tension components due to dispersive (London–van der Waals) and polar (Debye, Keesom–van der Waals, and acid-base) forces, respectively. Polar forces, expressed as a geometric mean, remain controversial, especially because the second term of the sum should theoretically be multiplied by a parameter that varies between 0.5 and 1, depending on the polarity of both phases. Equation 2 is thus valid only when the phases have similar polarities. However, this equation was widely used in numerous studies and has proved to be useful (13).

(ii) McGuire's model (4),

$$Wa = 2 \cdot \sqrt{\gamma_S^d \cdot \gamma_L^d} + \left(K \cdot \gamma_L^p + B\right) \qquad [3]$$

where K and B are constants for a given solid. This model is consistent with Dann's results (14) and has the advantage of not using the solid polar surface tension component γ_S^p, which is difficult to calculate accurately (5).

(iii) Wu's model (15):

$$Wa = 4 \cdot \frac{\gamma_L^d \cdot \gamma_S^d}{\gamma_L^d + \gamma_S^d} + 4 \cdot \frac{\gamma_L^p \cdot \gamma_S^p}{\gamma_L^p + \gamma_S^p} \qquad [4]$$

This empirical model expresses work of adhesion as a harmonic mean of dispersive and polar components of surface tension. It is meant to be used between a product of high surface energy and another of low surface energy, which is quite restrictive.

(iv) Van Oss *et al*. model (16),

$$Wa = 2 \cdot \sqrt{\gamma_L^{LW} \cdot \gamma_S^{LW}} + 2 \cdot \sqrt{\gamma_L^+ \cdot \gamma_S^-} + 2 \cdot \sqrt{\gamma_L^- \cdot \gamma_S^+} \qquad [5]$$

where γ^{LW} is the surface tension component due to all van der Waals forces (London, Debye, and Keesom). γ^+ and γ^- are, respectively, Lewis acid and base parameters of surface tension. The acid-base component γ^{AB}, for each product, is the geometric mean of γ^+ and γ^-. This model was useful to calculate adhesion of bacteria to surfaces involving acid-base interactions and electrostatics (17).

(v) Germain's model (18),

$$Wa = 2 \cdot \sqrt{\gamma_L^d \cdot \gamma_S^d} + 2 \cdot \sqrt{\gamma_L^p \cdot \gamma_S^p} + 2 \cdot \sqrt{\gamma_L^h \cdot \gamma_S^h} \qquad [6]$$

where γ^h is the surface tension component due to hydrogen bonds. It is differentiated from polar van der Waals forces (Debye and Keesom), which are included in γ^p only. This new model has been used to study the adhesion of inks to polymer surfaces (18).

No direct check of solids' surface tensions, used in these five models, is possible. Thus, from a food industry point of view, it is interesting to see if these adhesion models predict edible oil bulk adhesion residues well by comparing them to experimental adhesion results.

EXPERIMENTAL PROCEDURES

Oils and solid surfaces. Three edible oils were used: virgin olive oil (Puget, Vitrolles, France); refined first-draft sunflower oil (Lesieur, Neuilly, France), and soybean oil (Solior, Tourcoing, France). Pure, white vaseline oil (OSI, Maurepas, France) was also used as a chemical reference oil, for its quality and constant composition.

Four solid surfaces were chosen: low-density polyethylene (LDPE), polyethylene terephthalate (PET), stainless steel AISI #304, and glass, both for their use in food packaging and equipment and for their hydrophilicity or hydrophobicity. Parafilm® 'M' (American National Can, Neenah, WI) was used as a hydrophobic, apolar reference surface: γ_S^d = 25.5 $mN \cdot m^{-1}$ (19).

Standard liquids. Various standard liquids, of the highest purity available, were used to determine solid surface tensions. Apolar liquids were diiodomethane (Sigma, St. Louis, MO), α-bromonaphthalene, cyclohexane (Prolabo, Paris, France), *n*-hexane, and *n*-hexadecane (OSI). Polar liquids were distilled, deionized water (Chromanorm®, Prolabo), glycerol, formamide, ethylene glycol, and ethanol (OSI).

Viscosity. Viscosity of oils was measured at 20 ± 1°C with a Viscosimatic MS capillary viscometer (Fica c/o Sepema, Nozay, France):

$$\eta_{oil} = \eta_{water} \cdot \frac{\rho_{water}}{\rho_{oil}} \cdot \frac{t_{oil}}{t_{water}} \quad [7]$$

where η is Newtonian viscosity (mPa · s), ρ is density (kg · m^{-3}) measured with a 10-mL pycnometer, and t is the time (s) for the product to flow between two defined levels of the capillary.

Acidity. Oil acidity was determined as described in Reference 20 with 0.01 N NaOH. Acidity (%) was expressed as mL NaOH necessary to neutralize 1 g of oil. Vaseline oil acidity was also measured to check the validity of the experiment.

Surface tension. Surface tensions of oils and standard liquids were measured with a Krüss K10ST tensiometer (Hamburg, Germany), equipped with a platinum plate (Wilhelmy method). The platinum plate was cleaned with ethanol and distilled water, then burned red-hot between each measurement. Glass cups containing samples were first cleaned by rinsing and soaking 10 min in acetone (OSI), then rinsed with ethanol and distilled water and dried 10 min in an oven (110°C).

The DuNoüy ring method (21) was used to measure interfacial tension between apolar and polar standard liquids (γ_{aL}). Polar liquids' γ_L^d component was then calculated as follows:

$$\gamma_L^d = \frac{(\gamma_a + \gamma_L - \gamma_{aL})^2}{4 \cdot \gamma_a} \quad [8]$$

where γ_a is the apolar liquid surface tension and γ_L is the polar liquid surface tension. The thermostated tensiometer was placed in a chamber regulated at 20 ± 1°C. The device maximum error was 0.1 mN · m^{-1}. Ten measurements were performed for each surface and interfacial tension.

For ethanol solutions, γ_L^d could not be measured this way; therefore, it was calculated from contact angles on Parafilm®.

Solid surface cleaning. For a proper measurement of θ, solid and liquid must be in equilibrium, and the surface should be clean and homogeneous. Prior to each experiment, surfaces were cleaned with ethanol and soaked 30 min in a 4% RBS detergent bath (Société Traitements Chimiques des Surfaces, Lille, France). Surfaces were rinsed 1 min under running tap water, then rinsed with distilled water. They were finally dried 10 min in an oven at 110°C for stainless steel and glass or 45 min at 50°C for polymers (PET, LDPE).

Contact angles. A device that included a video camera coupled to image analysis was specially designed to measure contact angles (Fig. 2). Solid surfaces were placed on a sample holder in a Plexiglas box to protect drops from external perturbations. It was previously established that the Plexiglas did not induce optical distortions. Product drops (10 µL) were deposited through a septum with a square-cut tip syringe. The device was placed in a 20 ± 1°C thermoregulated chamber. The sample holder could be rotated to check if the contact angle was constant around the drop. Device horizontality was checked between each measurement.

Acquisition of liquid drop images was obtained with an image analysis video camera (Sony, Japan) with a 60-mm zoom lens (Nikkor®, Nikon, Japan) connected to a 512 × 512 pixel superfine pitch screen (Trinitron, Sony, Japan). Images were treated and digitized with Visilog® 3.6 software (Neosis Visron Inc., Montréal, Canada). A Fortran program was written to calculate contact angle. The program determined the top and edges of the drop and then calculated three angles: the theoretical contact angle and the two true contact angles on the right and left sides of the drop. For each oil and standard liquid, measurements of contact angles were repeated 10 times.

The validity of the contact angles obtained by the Fortran program was checked by scanning known geometrical figures with angles of 10, 15, 25, 45, 60, 70, and 75°. The program calculated the angles with a maximum error of 2° on larger angles. This confirms the validity of our image analysis method. This method has the advantage of not depending on visual accuracy. The method usually found in the literature to measure contact angles uses a goniometer. Even with some

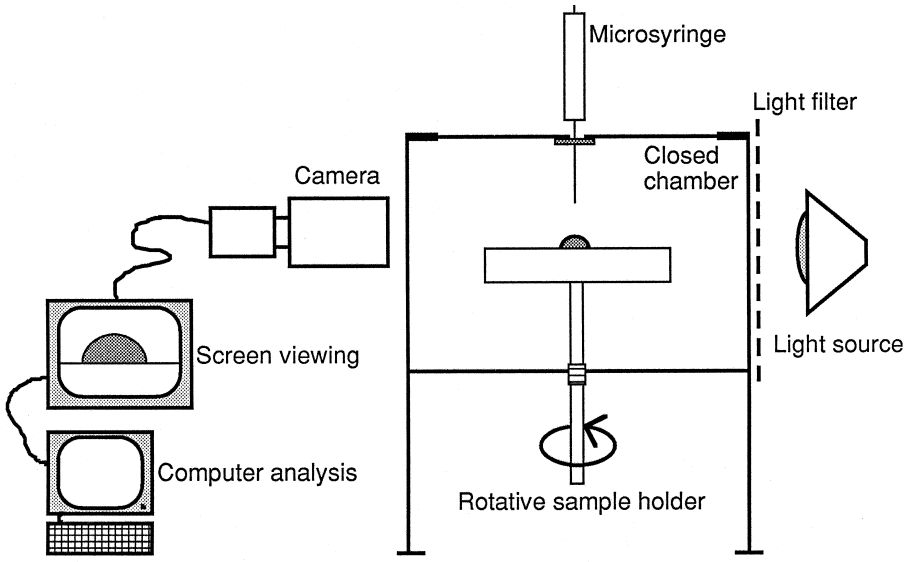

FIG. 2. Device for contact angle measurement by image analysis.

automatic goniometers, the operator has to define the angle on the screen. In our method, once pictures of drops are logged in, the program analyzes them all in the same manner, avoiding operator-induced errors.

Calculation of oil and solid surface tension components. A solid's surface tension as well as its dispersive, polar, acid-base, and hydrogen components may not be measured directly. They are calculated from contact angle measurements of standard liquids on the surfaces by using equations established from models previously described. For each model, the Young-Dupré equation is used for the left side of the equation, and the model expression for the right side. This usually gives the equation of a curve, the slope and Y-intercept of which give the desired surface tension components. For models involving more than two parameters, such as Equations 5 and 6, sets of equations are solved, with standard liquid pairs or triplets, to calculate the components (18,22).

The surface tension dispersive component of oils was determined from contact angles on Parafilm®. The polar component was deduced from the total surface tension:

$$\gamma_{oil}^{d} = \frac{\left[\gamma_{oil} \cdot \left(\cos\theta_{oil,Parafilm} + 1\right)\right]^2}{4 \cdot \gamma_{Parafilm}} \quad [9]$$

$$\gamma_{oil}^{p} = \gamma_{oil} - \gamma_{oil}^{d} \quad [10]$$

Other components (γ^{AB}, γ^{h}, γ^{-}, γ^{+}) were calculated from contact angles on solids previously characterized by solving sets of equations for each model, as described above.

Experimental measurements of oil adhesion. The bulk experimental adhesion (EA) of oils to surfaces was measured by a method set up in our laboratory (Fig. 3) and described by Ould Eleya and Hardy (23). It consists of putting 30 mL of product on top of an 80° tilted solid surface. The product is held back by a removable wall. The device is placed in a 20 ± 1°C thermoregulated chamber and the wall is opened to let the product flow down. The weight remaining on the solid surface after flow has stopped is measured, so that:

$$EA = \frac{\text{deposit weight}}{\text{active surface}}\left(g \cdot m^{-2}\right) \quad [11]$$

where deposit weight = solid weight after flow − solid weight before flow, and active surface = surface actually occupied by oil. The end of flow time is determined by recording oil weight dropping down during the experiment with a precision balance (Precisa 400M; PAG, Zürich, Switzerland). End of flow is determined as the point when less than 0.1 g of oil drops down during 15 min, at which point the mass of oil remaining on the plate is considered as constant. For each oil, the end of flow time was 1 h. The active surface was measured with a 1-mm precision ruler.

Each measurement with our EA device was run in triplicate. Low standard deviations (between 1 and 7%) for each oil on the different surfaces validated the method.

This method gives a measure of the global adhesion amount, i.e., adhesion plus cohesion strengths of the oil, and

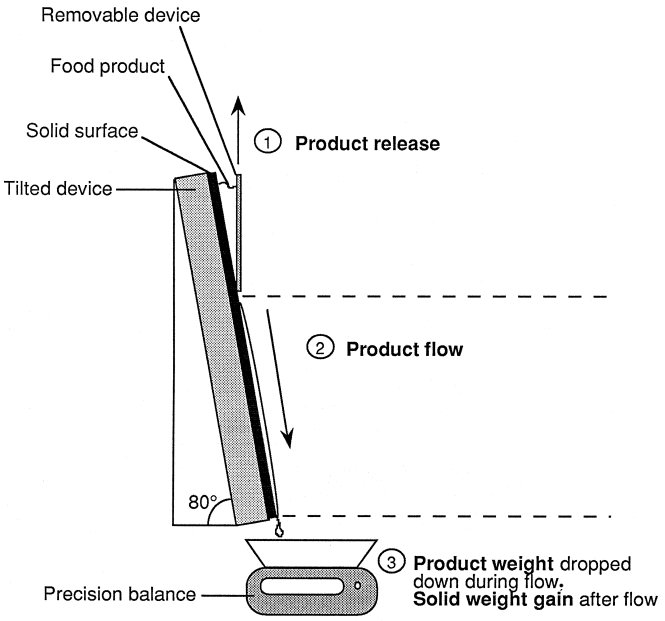

FIG. 3. Device for experimental adhesion measurement.

should not be interpreted as the true interfacial adhesion, which concerns only the first molecular layers on the solid. Indeed, the first molecular layers are attached to the solid by adhesive forces that decrease with distance, so that upper layers remain attached owing to the oil's own cohesive strength. Thus, different results may be interpreted as adhesion differences if compared for the same oil on various solids, but not if compared between different oils, because cohesion is then different (3). However, the advantage of this method is that it will allow us to see if this bulk adhesion amount remains correlated to the thermodynamic work of adhesion or if it is only due to hydrodynamic factors.

RESULTS AND DISCUSSION

Characterization of solids. Surface tensions of the standard liquids used to characterize the solids were in agreement with the literature (4,11,14,22; results not shown). Also, the contact angles of standard liquids on solid surfaces were close to those in the literature for the same type of solid (14,17,18,24; results not shown).

Solid dispersive and polar components of surface tension are given in Table 1. The dispersive components of all surfaces fall in the same range (30–40 $mN \cdot m^{-1}$). Lifshitz–van der Waals components, using the van Oss *et al.* method (16), were close to dispersive components given by other methods (Table 2).

Differences between solids were more likely due to the differences in their polar surface tension parameters than to the dispersive component. This polar parameter almost vanished for LDPE, while it was almost as important as the dispersive component for glass. Solids ranked in the following order of increasing polarity: LDPE < PET < stainless steel < glass, which is consistent with the literature (17,18,24). This order

TABLE 1
Polar and Dispersive Components of Solid Surface Tensions as Derived from Various Models (mN · m^{-1})[a]

	Calculation method (ref. no.)	γ^d	γ^p
LDPE	Owens and Wendt (12)	38[a]	0.3[a]
		35.2[b]	0.2[b]
	Wu (15)	37.4[a]	0.6[a]
	Germain (18)	31.5[a]	9.2[a]
		35.4[b]	0.5[b]
PET	Owens and Wendt	38.2[a]	4.8[a]
		41[b]	1.7[b]
	Wu	44.7[a]	23.9[a]
	Germain	33[a]	2[a]
		39.6[b]	0.9[b]
Stainless steel	Owens and Wendt	33.8[a]	6.2[a]
		35.5[c]	10.1[c]
	Wu	40.3[a]	28[a]
	Germain	30.9[a]	3.9[a]
		34.7[c]	8.2[c]
Glass	Owens and Wendt	29.3[a]	25.4[a]
		33[d]	26.5[d]
	Wu	37.4[a]	52.8[a]
	Germain	26[a]	14.8[a]

[a]Present study.
[b]Germain (18).
[c]Boulange-Peterman (17).
[d]Haudrechy (25). Abbreviations: LDPE, low-density polyethylene; PET, polyethylene terephthalate.

of material polarity was the same when using McGuire's K and Wa^p_{water} parameters (Table 2):

$$Wa^p_{water} \text{ is equal to } \gamma_{water} \cdot (\cos\theta + 1) - 2 \cdot \sqrt{\gamma^d_{water} \cdot \gamma^d_S}$$

reflecting the affinity between solid and water, and K is the slope of the McGuire model (Eq. 3), which increases with surface polarity (4,7).

Slight differences between our results and literature values must be due to the various solid compositions, especially for stainless steel and glass that may be of different types. The cleaning procedure may also have induced some residual polarity because we used ethanol and a detergent. Moreover, depending on the method, different test liquids were used, which may influence the results. However, because we used a variety of test liquids, this kind of distortion should be reduced.

TABLE 2
Solid Surface Parameters (mN · m^{-1}) Established by Models of Van Oss *et al.*, Germain and McGuire[a]

	γ^{LW}	γ^+	γ^-	γ^{AB}	γ^h	K	B	Wa^p_{water}
LDPE	36.9	1.1	0.25	1	4.1	0.21	−2.91	6.2
PET	44.7	0.05	14.3	1.7	11.1	0.98	−13.90	36.4
Stainless steel	40.1	0.2	19.3	3.9	13.4	1.06	−12.01	41.3
Glass	36.8	0.85	47.5	12.7	23.6	1.83	−15.36	78

[a]Van Oss *et al.* (16); Germain (18); McGuire (4). Abbreviations: see Table 1.

TABLE 3
Components of Oil Surface Tension (mN · m^{-1})[a]

	γ^d	γ^p	γ^{LW}	γ^+	γ^-	γ^h
Olive oil	31.4[x]	1.6[x]	31.4	0.66	0.97	
	32.8[y]	0.14[y]				0.04
Sunflower oil	33.6[x]	0[x]	33.6	0	0	
	32.9[y]	0.4[y]				0.3
Soybean oil	32[x]	1.5[x]	32	0.82	0.72	
	33.3[y]	0.2[y]				0.05
Vaseline oil	30.4[x]	0[x]	30.4	0	0	
	29[y]	0.9[y]				0.5

[a]Calculation method: [x]Owens and Wendt (12); [y]Germain (18).

Characterization of oils. Oils showed some degree of polarity because γ^p did not always vanish, except for sunflower- and vaseline oils in the Owens and Wendt (12) model. However, γ^p may be considered negligible because it never exceeded 5% of γ^d (Table 3). This residual polarity must be due to the presence of fatty acids; acidity was 2.2, 0.4, 0.5, and 0% for olive, sunflower, soybean, and vaseline oil, respectively. Overall, there were only small differences between the surface tensions of the different oils. Values of each type of surface tension component also fall in the same range for all oils. We may conclude at this point that possible major experimental adhesion differences between oils may come from their viscosity, composition, and properties of the solids in contact with them, rather than from surface tension differences of the oils.

Comparison of work of adhesion and EA. EA of oils correlated linearly to Wa (Fig. 4) as calculated from the Young-Dupré Equation [1]: $R^2 = 0.999$ for soybean oil, 0.988 for sunflower oil, 0.967 for olive oil, and 0.905 for vaseline oil. The Young-Dupré equation takes into account a bulk characteristic of the liquid (γ_L) as well as a component of the solid-liquid system (θ), both measurable with certainty. This proves

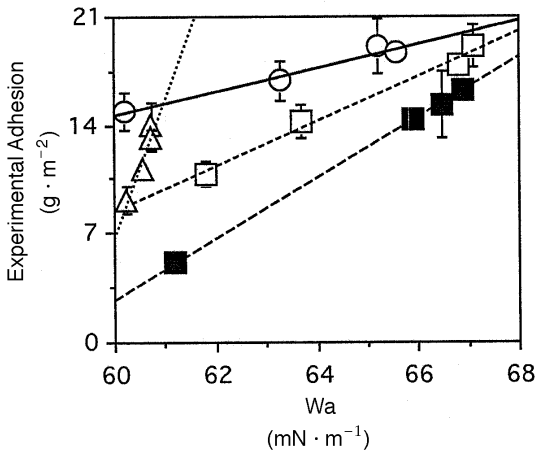

FIG. 4. Comparison of oil experimental adhesion with the work of adhesion as calculated with the Young-Dupré equation. ○, Olive oil; □, sunflower oil; ■, soybean oil; △, vaseline oil.

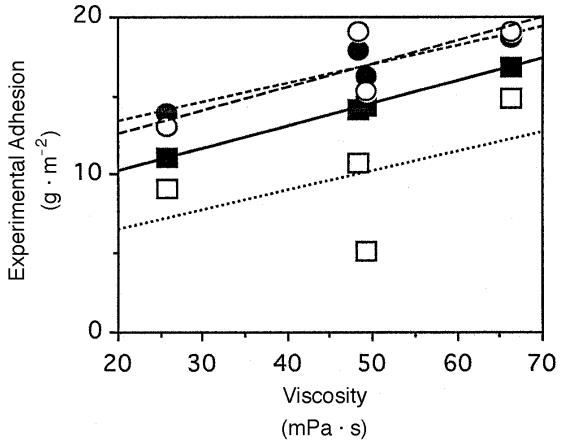

FIG. 5. Effect of oil viscosity on experimental adhesion. ■, Stainless steel; □, glass; ●, polyethylene terephthalate; ○, low-density polyethylene.

the importance of thermodynamic adhesion in oil interactions with packaging and equipment surfaces, even if the bulk residual weight is not a function of interfacial contact alone. Slope differences between different oils suggest the importance of other factors that influence flow. However, as EA increases with Wa, there is certainly no equally important parameter leading to the converse trend. Other adhesion causes such as surface rugosity (mechanical adhesion) and rheology should still be investigated, to improve understanding of adhesion differences for different surfaces and products. For instance, EA increased with oil viscosity (Fig. 5). Indeed, viscosity limits flow and results in greater thickness and heavier weight of remaining deposits. No particular relationship was found between oil density and adhesion, certainly because densities varied in a narrow range (0.86–0.94). Nevertheless, we suggest that density should limit remaining deposits owing to gravitational forces.

Effect of solid surface properties on experimental adhesion. Solid characteristics also acted on EA, because we observed a linear decrease of oil EA with surface hydrophilicity estimated by Wa^p_{water} (Fig. 6). Moreover, EA decreased with

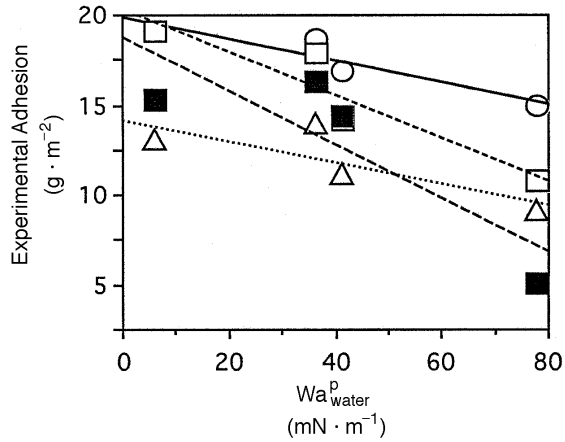

FIG. 6. Effect of surface hydrophilicity on oil experimental adhesion. ○, Olive oil; □, sunflower oil; ■, soybean oil; △, vaseline oil.

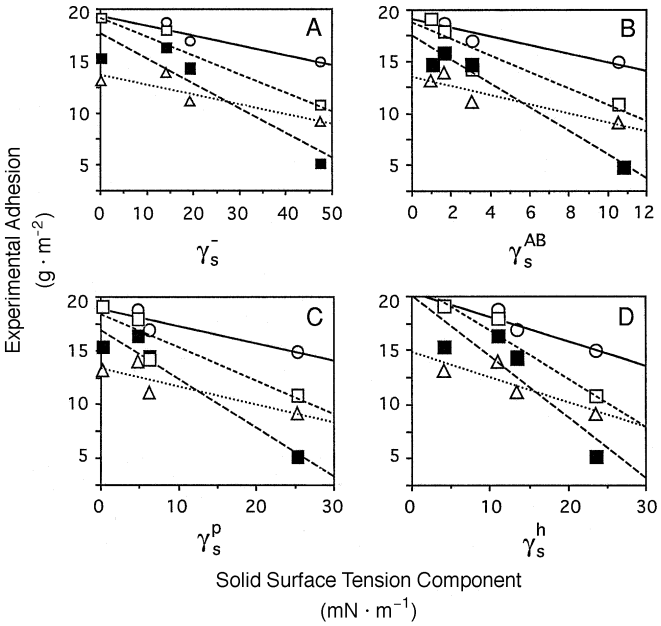

FIG. 7. Effect of surface polarity, as calculated by polar, acid-base, or hydrogen surface tension components, on oil experimental adhesion. (A,B) van Oss *et al.* (16) method, (C) Owens and Wendt method (12), (D) Germain method (18). ○, Olive oil; □, sunflower oil; ■, soybean oil; △, vaseline oil.

surface polarity based on γ_S^p, γ_S^{AB}, and γ_S^h (Fig. 7). EA also decreased with γ_S^-, suggesting that oils have a slight hydrogen-donor trend (confirming the results in Table 3). The presence of residual fatty acids can explain this observation. Conversely, EA increased with the nonpolar character (estimated by γ_S^d) of the surface (Fig. 8). Moreover, for each adhesion model, Wa was composed of at least 80% of dispersive interactions (first term of the sum in Equations [2–6]), which is consistent for such hydrophobic products.

Correlation between adhesion models and experimental adhesion of edible oils. EA and Wa, calculated for each oil by McGuire and Germain Equations [3 and 6], correlated well (Fig. 9): R^2 ranged between 0.751 and 0.946 for McGuire and 0.751 and 0.970 for Germain. McGuire's model separates polar and dispersive components of surface tensions but does

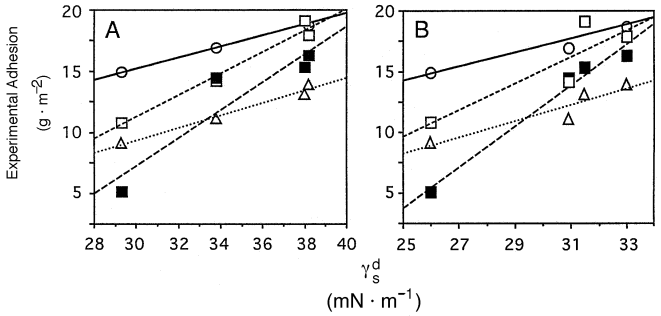

FIG. 8. Effect of surface apolarity, as calculated by dispersive surface tension component, on oil experimental adhesion. (A) Owens and Wendt method (12), (B) Germain method (18). ○, Olive oil; □, sunflower oil; ■, soybean oil; △, vaseline oil.

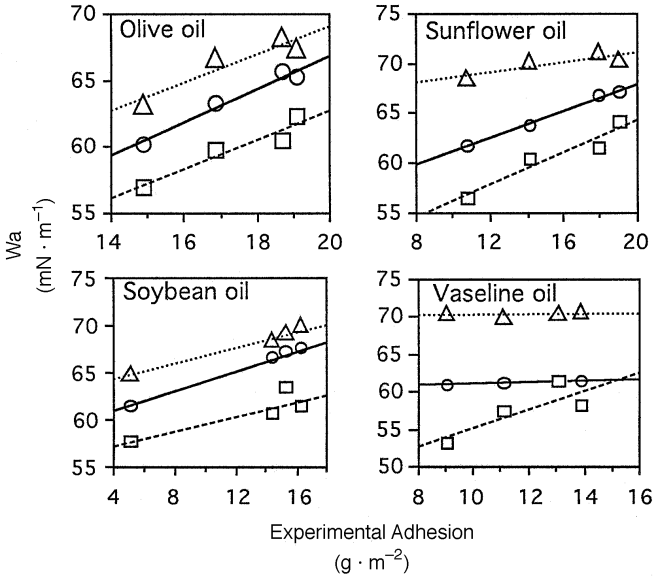

FIG. 9. Comparison of the work of adhesion, by different models, with oil experimental adhesion. ○, Young-Dupré (9,10); □, McGuire (4); △, Germain (18).

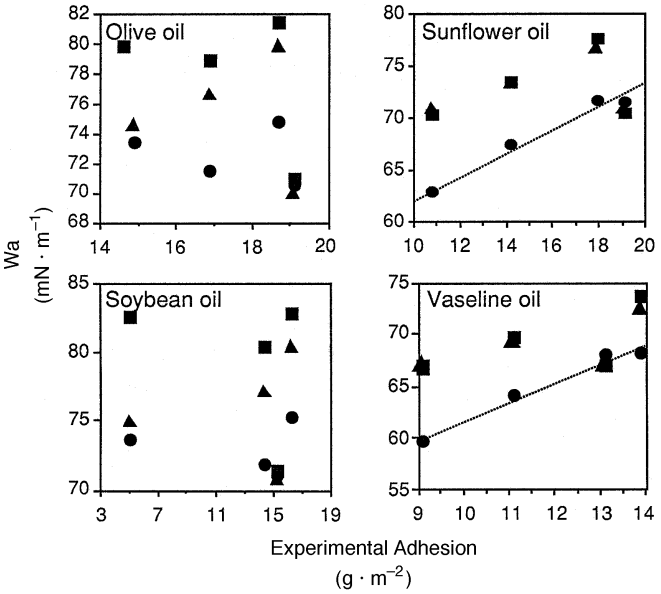

FIG. 10. Models that do not correlate well with oil experimental adhesion. ●, Owens & Wendt; ▲, Wu; ■, van Oss *et al.*

not take γ_S^p into account, which is considered as not a reliable parameter (4). This approach seems to be efficient in predicting bulk adhesion in oils. The efficiency of this method in our case is certainly due to the nonpolar character of oils because the geometric mean term, including γ_L^p, is very low. Germain's model also seems to be consistent for our particular products. This may be due to the splitting of long-range van der Waals forces that are associated with neither dispersive nor acid-base forces. Indeed, this method gave better results than other models, such as the geometric mean or acid-base approaches. For each correlation, the three edible oils have almost the same behavior, whereas vaseline oil always behaves differently. This shows the influence of oil composition on top of rheological or surface parameters. This pure chemical oil therefore should not be used to model experimental adhesion of edible oils.

Other methods did not correlate to EA for any oil (Fig. 10). The apparent inadequacy of the van Oss *et al*. method (Eq. [5]) for bulk adhesion of edible oils must be due to the low γ^+ and γ^- (proton-donor and acceptor component) values of oils. The same remark can be made about the Owens and Wendt model (Eq. [2]). In this case, polar components of the surface tension take on the same role as dispersive ones in the calculations, even though polar interactions are not important for oils. It should be noted that the Owens and Wendt model seemed to correlate with sunflower and vaseline oils' EA (lines in Fig. 10). However, the polar component of these oils vanishes (Table 3). Thus, only the Fowkes geometric mean of dispersive components actually remains, which is not specific to this model. The Van Oss *et al.* model also seemed to fit better for these oils than for olive and soybean oils, certainly because γ^+ and γ^- of sunflower and vaseline oils also vanish, so that only γ^{LW} is used. Wu's model (Eq. 4) may be inappropriate in our experiments owing to the use of polymers along with glass and stainless steel. Theoretically, this model is valid for high-surface-energy solids with low-energy liquids.

Overall adhesion differences between vaseline and edible oils show that substrate purity and origin (natural or chemical) is of importance in adhesion phenomena. Chemical oils do not give any insight on edible oil behavior. Thus, adhesion predictions applied to food materials cannot be derived from pure chemical products, and bulk adhesion follows more complex laws. However, it seems that some of the theoretical adhesion models can be applied to estimate bulk adhesion values for edible oils reliably. Particularly, knowledge of the oils' surface tension and contact angle on solids allows a simple and reliable estimation of food-to-solid adhesion. This study thus impacts on food technology, concerning both food packaging and surface cleaning problems. The prediction of adhesion residues can help in choosing an appropriate packaging material for particular oils or fatty products to limit residual product in the package after consumption. Also, choosing a particular surface treatment or coating for industrial equipment surfaces can reduce cleaning costs.

REFERENCES

1. Lai, C.C., Sticky Problems in Food Packaging, in *Food Product-Package Compatibility*, edited by J.I. Gray, B.R. Harte, and J. Miltz, Technomic Publishing Co., Lancaster, PA, 1987, p. 258.
2. Checkmareva, I.B., V.G. Babak, and R.I. Dzhafarova, Prevention of Adhesion of Margarine Emulsion to Surfaces of Technological Equipment, *Izv. Vyss. Ucebn. Zaved. Pis. Technol. 2*: 3–36 (1985).
3. Michalski, M.C., S. Desobry, and J. Hardy, Food Materials Adhesion: A Review, *CRC Crit. Rev. Food Sci. Nutr. 37*:591–619 (1997).
4. McGuire, J., and S.A. Kirtley, Surface Characterization for Prediction of Food Particle Behavior at Interfaces: Theoretical Considerations and Limitations, *J. Food Eng. 8*:273–286 (1988).

5. McGuire, J., and S.A. Kirtley, On Surface Characterization of Materials Targeted for Food Contact, *J. Food Sci. 54*:224–226 (1989).
6. McGuire, J., On Evaluation of the Polar Contribution to Contact Material Surface Energy, *J. Food Eng. 12*:239–247 (1990).
7. Krisdhasima, V., J. McGuire, and R. Sproull, Surface Hydrophobic Influences on β-Lactoglobulin Adsorption Kinetics, *J. Colloid Interface Sci. 154*:337–350 (1992).
8. Boulange-Peterman, L., B. Baroux, and M.N. Bellon-Fontaine, The Influence of Metallic Surface Wettability on Bacterial Adhesion, *J. Adhes. Sci. Technol. 7*:3 (1993).
9. Young, T., An Assay on the Cohesion of Fluids, *Phil. Trans. Roy. Soc. 95*:65–87 (1805).
10. Dupré, A., *Théorie Mécanique de la Chaleur*, edited by Gauthiers-Villars, Paris, 1869.
11. Fowkes, F.M., Attractive Forces at Interfaces, *Ind. Eng. Chem. 56*:40–52 (1964).
12. Owens, D.K., and R.C. Wendt, Estimation of the Surface Free Energy of Polymers, *J. Appl. Polym. Sci. 13*:1741–1750 (1969).
13. Kinloch, A.J., Review. The Science of Adhesion. Part 1. Surface and Interfacial Aspects, *J. Mater. Sci. 1980*:2141–2166 (1980).
14. Dann, J.R., Forces Involved in the Adhesive Process. I. Critical Surface Tensions of Polymeric Solids as Determined with Polar Liquids, *J. Colloid Interface Sci. 32*:2, 302–331 (1970).
15. Wu, S., Polar and Nonpolar Interactions in Adhesion, *J. Adhes. 5*:39–51 (1973).
16. Van Oss, C.J., M.K. Chaudhury, and R.J. Good, Interfacial Lifshitz–van der Waals Interactions in Macroscopic Systems, *Chem. Rev. 88*:927 (1988).
17. Boulange-Peterman, L., Etude physico-chimique et électrochimique de l'adhésion de *Leuconostoc mesenteroides* et *Streptococcus thermophilus* à des surfaces d'acier inoxydable, Ph.D. Thesis, Université de Nancy I, France, 1993.
18. Germain, C., Caractérisation superficielle d'encres et de polymères dans le but de prévoir leur adhérence, Ph.D. Thesis, Université Lyon I, France, 1994.
19. Busscher, H., Surface Free Energies and the Adhesion of Oral Bacteria, Ph.D. Thesis, University of Gröningen, Netherlands, 1985.
20. *Official Methods of Analysis,* 15th edn., edited by Association of Official Analytical Chemists, Inc., Arlington, 1990, p. 957.
21. Harkins, W.D., and H.F. Jordan, A Method for the Determination of Surface and Interfacial Tension from the Maximum Pull on a Ring, *J. Am. Chem. Soc. 52*:1751–1772 (1930).
22. Van Oss, C.J., R.J. Good, and H.J. Busscher, Estimation of the Polar Surface Tension Parameters of Glycerol and Formamide, for Use in Contact Angle Measurements on Polar Solids, *J. Dispers. Sci. Technol. 11*:75–81 (1990).
23. Ould Eleya, M., and J. Hardy, Evaluation of the Food Adhesion onto Packaging Materials, *Food Preservation 2000,* Proceedings of a Conference held at Science and Technology Corporation, Hampton, VA, U.S. Army Natick Research, MA, October 19–21, 1993, p. 877.
24. Bellon-Fontaine, M.N., Caractérisation physico-chimique des surfaces solides γ_s et adhésion des bactéries aux surfaces, Ph.D. Thesis, Université Pierre et Marie Curie, Paris, 1986.
25. Haudrechy, P., Caractérisation des interactions physico-chimiques entre les surfaces de verre et vitrocéramique et l'alpha-lactalbumine en solution, Ph.D. Thesis, Université des Sciences et Techniques de Lille Flandres Artois, Lille, France, 1990.

[Received June 9, 1997; accepted November 5, 1997]